Journal of GeoEngineering, Vol. 15, No. 4, pp. 205-214, December 2020
http://dx.doi.org/10.6310/jog.202012_15(4).4

Case Study:

CASE RECORD OF PHASE 1 OF KAOHSIUNG METRO – GEOTECHNICAL DESIGN AND CONSTRUCTION OF A LARGE-SCALE UNDERGROUND STATION

Bin-Chen Benson Hsiung [1*], Li-Jung Chung [2], and Miao-Chi Lin [3]

ABSTRACT

This paper mainly aims to describe details of a large- scale strut-free cofferdam excavation with a diameter of 140 m and a depth of 27 m. The excavation was performed as part of the construction of an interchange station in Phase 1 of the Kaohsiung MRT system and it includes aspects of geotechnical engineering design, construction and performance of said excavation in this paper. The pit was retained by a 1.8 m thick, 60 m deep reinforcement concrete diaphragm wall only without additional support. A circular-shaped cofferdam excavation was proposed so the hoop effect of the excavation is eligible to reduce displacement induced. Further, the wall toe was penetrated into impermeable clay layer which also leads to less impacts on adjacent ground outside the excavation. Observations of the excavation were reported. Numerical simulations of pumping and induced ground displacements of the cofferdam excavation suggested that the current parameters and scheme used can properly simulate changes in pore pressure during pumping. However, an advanced constitutive model considering small-strain soil behaviour should be adopted for ground displacement simulations and the reliability of monitoring ground movement data should be concerned due to reasons of instrument installation and survey error on main roads.

Key words: Sand, strut-free cofferdam excavation, observations, numerical simulations.

1. INTRODUCTION

Kaohsiung, which has a population of approximately 2.7 million, is the political and economic centre of southern Taiwan. However, the city is limited by a very poor public transportation infrastructure, and thus, most people must rely on cars and motorbikes for daily transportation purposes.

For these reasons, phase 1 of the Kaohsiung Mass Rapid Transit System (KMRTS; Kaohsiung Metro) was designed to fulfill the needs of the city. This paper firstly describes the project background of this system briefly. In addition, the design, construction and performance of a cofferdam excavation with a diameter of 140 m and a depth of 27 m used for the interchange station will be examined. Numerical analyses of pumping and ground displacement simulations of the cofferdam excavation are also included. A full picture of the accumulated experience in this work has not been reported previously, and the case record reported here is expected to be a useful reference for similar excavations with similar ground conditions in the future.

2. PROJECT BACKGROUND

To enhance the development of the city, a modern metro system was constructed in Kaohsiung, Taiwan. Phase 1 of the KMRTS consists of two lines, namely, the north-south Red Line and the east-west Orange Line. Figure 1 presents the network of phase 1 of the KMRTS. The total network length for phase 1 of the KMRTS, which includes 37 stations and three depots, is 42.7 km; of this network, 34.2 km must be constructed underground, including 27 stations and bored tunnels connecting the stations.

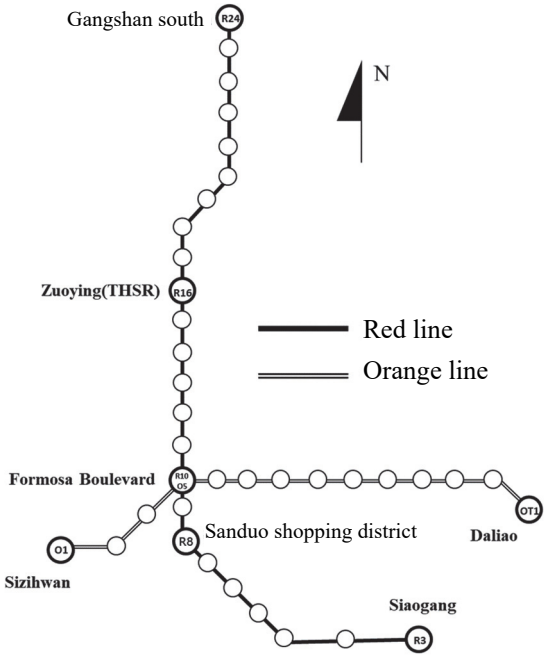

Note: "THSR" means also the station for Taiwan High Speed Rail

Fig. 1 Network of phase 1 of KMRTS

Manuscript received January 23, 2019; revised August 21, 2020; accepted September 17, 2020.

[1*] Professor (corresponding author), Department of Civil Engineering, National Kaohsiung University of Science and Technology, Kaohsiung City Taiwan (e-mail: benson@nkust.edu.tw).

[2] Former Deputy Director of General, Kaohsiung Mass Rapid Transit Engineering Bureau, Kaohsiung City, Taiwan.

[3] Division Chief, Kaohsiung Mass Rapid Transit Engineering Bureau, Kaohsiung City, Taiwan.

The general ground conditions are addressed first. Kaohsiung is located at the mouths of three main rivers: Dien-Bao River to the north, Love River in the centre and Cian Jhen River to the south. Thus, the ground for the underground section of the Red Line (which begins at station R3 in the south and ends at the north portal at station R16) mainly consists of soft alluvium except for the tunnel located to the north of Zuoying (station R16), which was constructed in limestone. Similarly, the stations and tunnels for the underground section of the Orange Line were also constructed in soft alluvium. Figure 2(a) presents the overall ground conditions of the underground section of the Red Line and the surface level of the underground section of Red Line was laid at an elevation level (EL.) ranging from approximately 5 to 20 m.

The ground conditions along the east-west Orange Line are similar to those along Red Line, and the ground mainly consists of silty sand and clay. The entire Orange Line was constructed underground except for one surface depot and a single above-ground station in the depot. The surface level of the ground along the line changes very little from an EL. of approximately 0 m at the seaside to the west to an EL. of 15 m on the hillside opposite the sea to the east. The ground water level is 0.5 m below the surface level in the west and gradually drops to 8 m below the surface level in the east far from the seaside. Furthermore, the water level exhibits a more significant change throughout the area closer to the sea due to the impact of the Earth's tide.

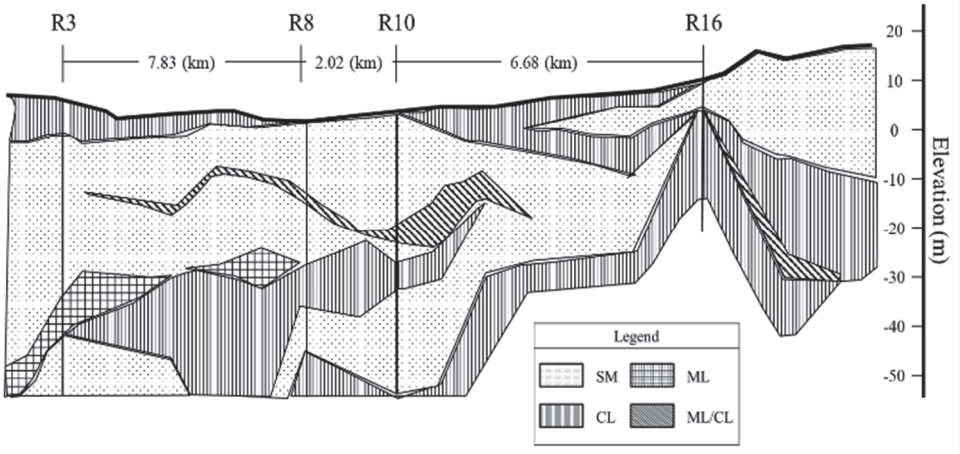

Note: "SM" means "Silty Sand", "ML" means "Low plasticity Silt" and "CL" means "Low plasticity Clay"

(a) Overall ground condition of underground section of Red Line

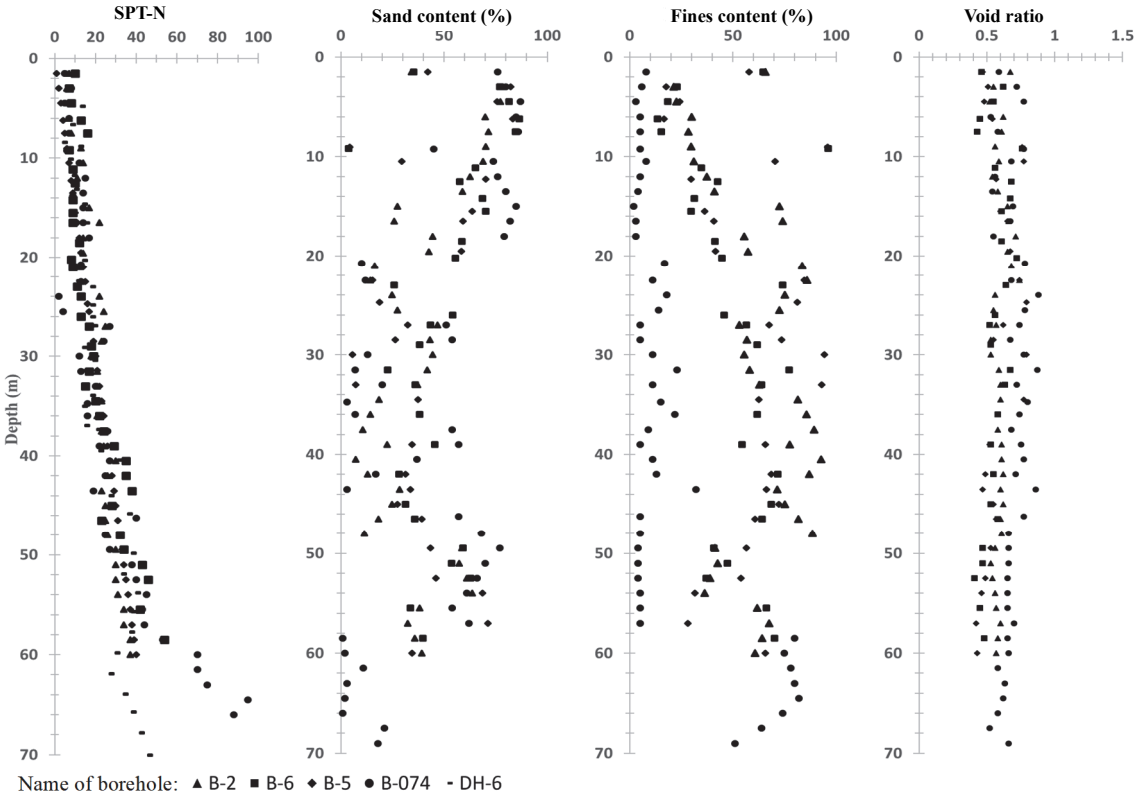

(b) Soil logs from 5 selected boreholes located close to O5/R10 station

Fig. 2 Representative ground condition of phase 1 of KMRTS and borehole log data obtained from O5/R10 site

3. CASE STUDY: AN EXTREME LARGE-SCALE COFFERDAM EXCAVATION

3.1 Design

To effectively connect the Red Line and Orange Line, an interchange station named "Formosa (O5/R10)" has to be designed and constructed, and thus, the construction of this station is critical.

Figure 2(b) shows the data from soil logs of boreholes located close to station O5/R10. As presented in Fig. 2(b), the soil material covering the ground is composed of mainly silty sand, silt and clay. The sand content is generally very high and ranges from approximately 75 to 95%; consequently, the fines content is much smaller from surface level up to 20 m below surface level, but the fines content increases once the ground goes deeper. The void ratio ranges from approximately 0.5 to 1.0. The standard penetration test (SPT-N) value of sand above the depth of the final excavation level is generally less than 30, which means that the materials are comparatively loose with a high permeability; moreover, the SPT-N value generally increases in proportion to an increase in the ground depth, which is consistent with the conclusion reached by Skempton (1986). In addition to the details shown in Fig. 2(b), the unit weight of the soil ranges from approximately 19.8 to 20.4 kN/m^3. Furthermore, the ground water level varies in the range from 3 to 4.6 m below the surface level. Above the final excavation level, the ground is mainly interbedded with several layers of silty sand and silt, but the wall toe penetrates into impermeable clay.

Because excavation is intended to take place over a large area to accommodate more passengers in the station, the use of a heavy strut system with polygon-shaped excavation does not seem to be very economical, and it could prolong the excavation time. Therefore, a circular-shaped cofferdam excavation was proposed. Considering the hoop (arching) effect formed by a circular excavation, a strut-free excavation is possible. At the beginning, an excavation with a diameter of 105 m was designed but the diameter increased to 140 m at the end to accommodate more passengers (refer to Figure 3a for layout of the excavation). Locations of selected instruments for data used in this study, such surface settlement indicators (SSI) and inclinometers in diaphragm wall (SID) are presented in Fig. 3(a) also. The maximum excavation depth reaches 27.1 m, and the pit was retained by a 1.8-m-thick, 60-m-deep diaphragm wall. An extra ring beam was constructed on top of the wall. Please refer to Fig. 3(b) for ground profile and cross section of the excavation.

Puller (2003) previously discussed examples about large-scale circular cofferdam excavations, which were adopted for metro projects in other places around the world, but similar cases have not been used in any urban underground excavation in Taiwan, where the ground is especially soft and highly permeable with a high ground water level. Therefore, substantial attention has been paid to related risks and impacts on the excavation and on the adjacent ground and structures. Similar to the procedure recommended by Clayton (2001), the risks related to the construction activities are categorized into three levels instead of four, namely, low, medium, and high levels of risk, which are associated with an event's likelihood and severity. Risk assessments of the excavation were consequently delivered. Through the assessment, high-level risks include (1) an unexpected eccentric load on the retaining wall from the soils, (2) defects or long delays in the retaining wall construction, (3) additional drawdown of the ground water

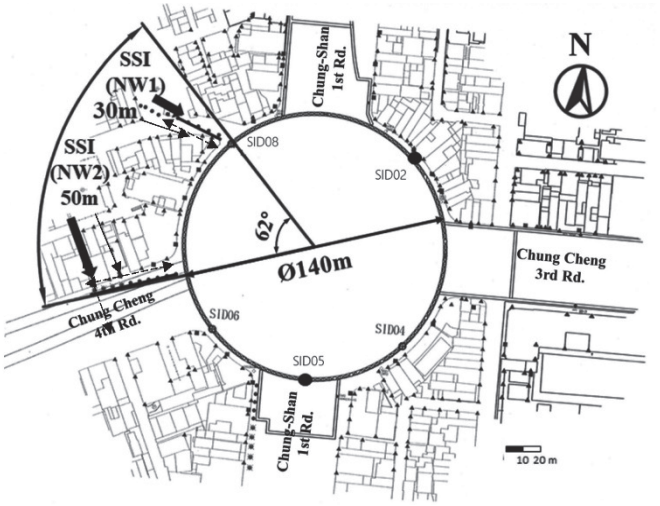

- SID: Inclinometer in diaphragm wall
- SSI: Surface settlement indicator

(a) Layout and locations of inclinometers in diaphragm wall (SID) and surface settlement indicators (SSI) of the excavation of O5/R10 station

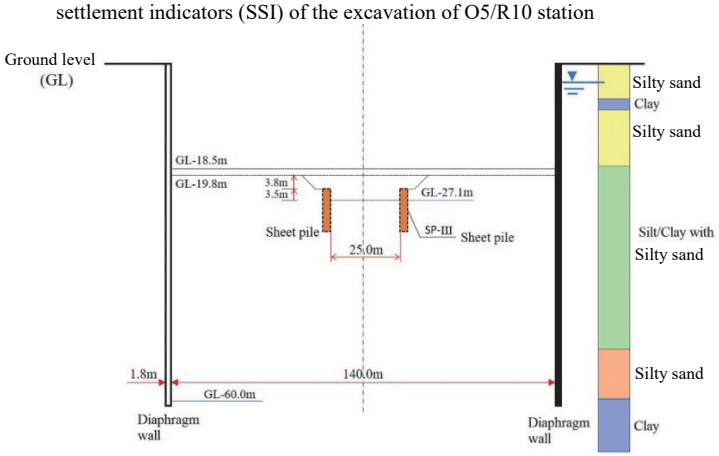

(b) Ground profile and cross section of cofferdam excavation of O5/R10 station

Fig. 3 Layout, location of selected instrument, ground profile and cross section of cofferdam excavation at O5/R10

level outside of the excavation zone, (4) launching of the tunnel boring (shield) machine and (5) excessive water ingress from leakage of the wall or unexpected large displacements of the wall.

3.2 Construction

To construct the retaining wall of a circular cofferdam, it is important to maintain a high-quality, fully rounded wall to retain the pit shape, because it constitutes the only support for the entire excavation. Therefore, a special machine known as an EXM with a special rotation cutter (or named "trench cutter) to be used for the diaphragm wall construction is presented in Fig. 4. The construction sequence, field conditions and temporary decking slab of the site are presented in Table 1 and Fig. 5. To fully retain the soils without any additional support, the wall must be constructed to be sufficiently stiff. Therefore, a very thick diaphragm wall using high-strength concrete (an unconfined compression strength of 42 MPa) with a ring beam on top has to be constructed. The wall was constructed panel by panel. However, there is no joint between any two panels due to the special shape at the panel junctions in contrast to common engineering practice in Taiwan. Temporary decking slabs were supported by vertical kingposts with lateral steel

Fig. 4 EXM and similar trench- cutter machines used for diaphragm wall construction of O5/R10 station

Table 1 Construction sequence of excavation and permanent structure of O5/R10

Phase number	Construction activities
1	Construct 1.8 m thick, 60 m deep diaphragm wall
2	Install Kingpost and temporary decking slab on surface for traffic diversion
3	Dewater and excavate to 4.0 m below ground surface
4	Dewater and excavate to 10.0 m below ground surface
5	Dewater and excavate to 13.0 m below ground surface
6	Dewater and excavate to 19.5 m below ground surface
7	Dewater and excavate to 23.5 m below ground surface level and install temporary retaining structure by sheet pile in central excavated zone
8	Dewater and excavate to 27.0 m below ground surface level; start to construct slab at B2F
9	Construct slab at B3F at central part and also complete construction of slab at B2F outer ring part of the excavation
10	Construct and complete slab at B1F which used for launching of shield machine at Southwest end of cofferdam; limited excavation activities were started up to the same depth of B1F in order to connect excavation zones using traditional strutting system
11	Continue to complete the permanent structure of B1F and transition zones connected to excavation zones using traditional strutting system
12	Complete the permanent structure at transition zone and construct permanent structures of top slab and accompanied facilities, such as entrances and ventilation shafts
13	Complete the permanent structure of the whole station and also accompanied facilities

bracings for temporary traffic diversion purposes. During the excavation, in principle, excavation activity is excluded or severely limited outside of the excavation zone to ensure that the functionality of the arching effect remains so that soils can still be retained without any additional support.

3.3 Performance

As indicated previously, it is important to maintain the fully rounded shape of the excavation throughout the construction process because it is strut-free. Therefore, monitoring is highly important for the construction as well as the revision of the design if necessary. To understand the performance during the excavation, instruments are installed on-site that are similar to those in other excavations performed during phase 1 of the KMRTS project.

Excessive wall movements are considered a key issue during construction. Wall displacements measured using various inclinometers are presented in Fig. 6, which shows the wall displacements at various excavations stages from 2 selected inclinometers in the wall (SID2 and SID5). The wall moves laterally, and the

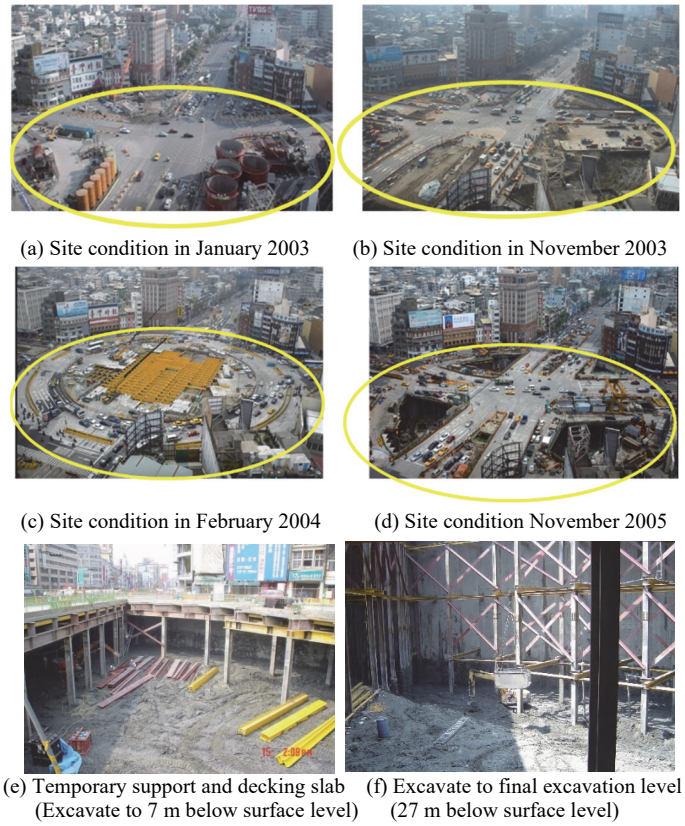

(a) Site condition in January 2003 (b) Site condition in November 2003

(c) Site condition in February 2004 (d) Site condition November 2005

(e) Temporary support and decking slab (Excavate to 7 m below surface level) (f) Excavate to final excavation level (27 m below surface level)

Note: circle in yellow means where the cofferdam is.

Fig. 5 Site condition of excavation at O5/R10 station

displacement gradually increases to 30 mm at the end of the excavation. A bulging wall deflection was observed throughout the entire excavation procedure, although the depth with the maximum wall displacement did not move significantly. It is believed that the ring beam at the top of the wall provided a comparatively stronger arching effect, which inhibits the displacements at the top of the wall. The ratio of the maximum wall displacement (δ_{hm}) to the maximum excavation depth was 0.11%, which seems to be lower than the range reported by Yao (2005), In addition to the arching effect from the cofferdam excavation, the thicker wall with a longer embedded depth might have been the reason for the observed reduction in the displacements. The higher concrete strength used to stiffen the wall may also have led to a small displacement. Another potential cause is the use of an excavation machine (EXM; trench-cutter machine) other than the hydraulic-grab machine commonly adopted in Taiwan for the construction of retaining walls, but further confirmation is required since data from other cases using EXM in similar ground conditions are lacking.

Based on data collected from rectangular excavations under similar ground conditions but with reinforced concrete retaining walls constructed by a hydraulic-grab machine and supported by H-type steel as a lateral support system, Hsiung (2020a) presented a non-dimension surface settlement trough. The ratio of the maximum surface settlement to the excavation depth may be up to 0.2%, and the influence zone can extend to 2.5 times the excavation depth. However, the distance of the influence zone is strongly related to the relative depth of the wall toe, pumping well and impermeable soil layer. Therefore, in the present case, surface settlement data are collected and compared with the observations of Hsiung (2020a).

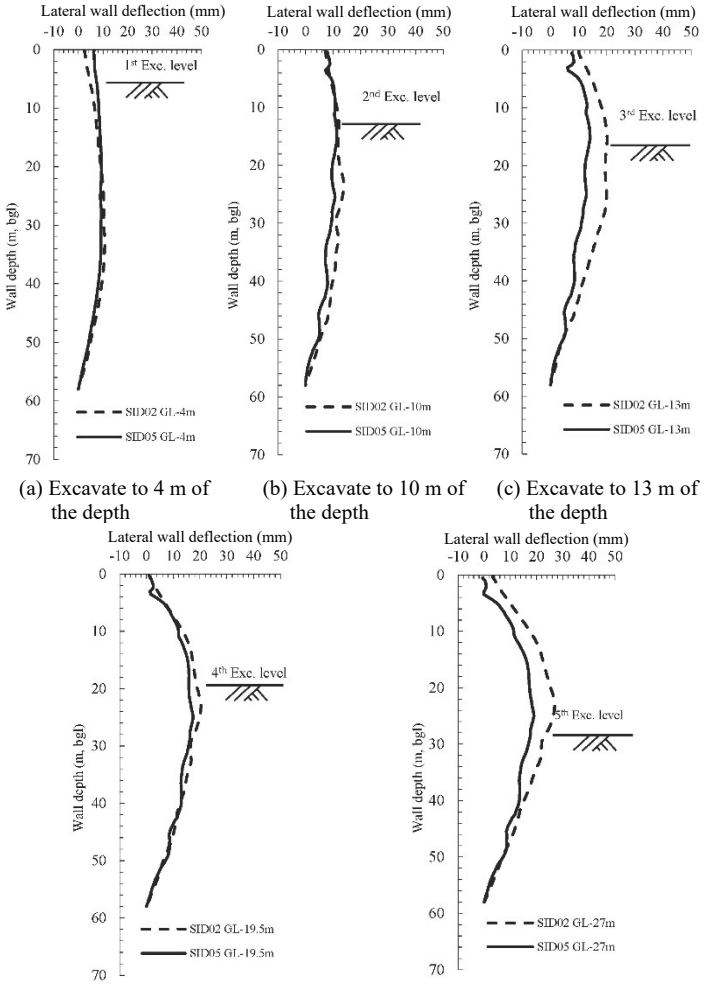

(a) Excavate to 4 m of the depth (b) Excavate to 10 m of the depth (c) Excavate to 13 m of the depth

(d) Excavate to 19.5 m of the depth (e) Excavate to 27.0 m of the depth

Fig. 6 Observed wall displacements at various stages from different inclinometers at O5/R10 excavation

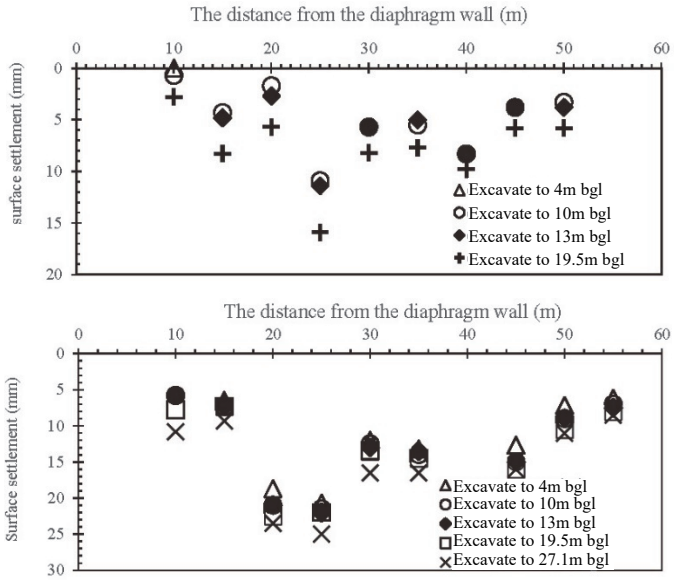

(a) Excavation induced surface settlement measured at various stages from selected sections (SSI-NW1 and SSI-NW2) (note: "bgl" means "below ground level")

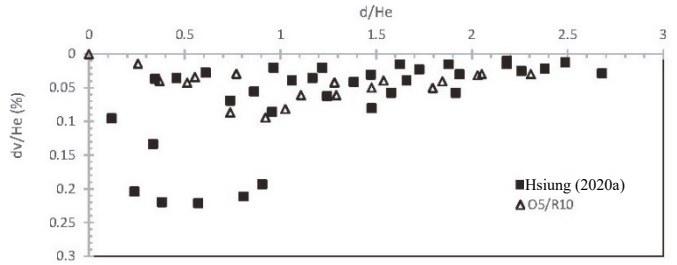

(b) Comparison of settlement trough from O5/R10 station excavation to settlement trough caused by excavation in Kaohsiung reported by Hsiung *et al.* (2020a)

Fig. 7 Measured surface settlement trough and also a comparison of settlement trough with data collected from other cases in Kaohsiung

Figures 7(a) and 7(b) first presents the measured surface settlement at various stages from selected sections. The maximum surface settlement (δ_{vm}) gradually increases from 17 mm to almost 28 mm at a location approximately 25 m from the excavation and remains at this location from the beginning to the end of the excavation. The hoop effect caused by cofferdam excavation is believed to be responsible for the persistence of the maximum surface settlement at the same location. In addition, limited surface settlements were measured (less than 10 mm) at approximately 55 m from the excavation, which is approximately 2 times the maximum excavation depth. The measured data from the final excavation stage were further interpreted and mapped into a plot by Hsiung (2020a), as shown in Fig. 7(c). This cofferdam excavation seems to induce smaller surface settlement as well as a smaller influence zone. It is likely that the reasons stated above are also applicable to the smaller surface settlement induced. Furthermore, the wall is embedded in comparatively thicker cohesive (silty and clayey) materials in deeper ground, which is anticipated to reduce the influence zone, consistent with the conclusions of Hsiung (2020a).

Effectiveness of the use of EXM rather than hydraulic- grab machine for impacts on surface settlements is also evaluated. Similar to discussions in lateral wall displacement, further validation is required since data from other cases using EXM in similar ground conditions are lacking.

The measured surface settlement data are also compared with the settlement envelope suggested by Clough and O'Rourke (2003), who indicated that the maximum settlement occurs very close to the excavation and that the influence zone is approximately 2 times the excavation depth. The location with the maximum surface settlement identified by Clough and O'Rourke (2003) differs greatly from that in a large-scale strut-free cofferdam excavation. As explained previously, due to the hoop effect, the location of the maximum surface settlement may be a certain distance away from the excavation instead of immediately next to the excavation. Moreover, sand-silt mixed ground might also influence the shape of the surface settlement trough caused by the excavation. However, the influence zone fits the conclusion of Clough and O'Rourke (2003) but should be related to the relative depth of the wall toe, pumping well and impermeable layer, as indicated by Hsiung (2020a). Furthermore, surface settlement at the ground beyond 2 times the maximum excavation depth was not monitored, and thus a further study to validate its consistency with the conclusions of Clough and O'Rourke (2003) about the influence zone will be carried out in the future.

The ratio of δ_{vm} to δ_{hm} is almost equal to 1, which is close to the value obtained from excavations in clay (Ou *et al.* 1993) but less than the values obtained from excavations in Kaohsiung

(Hsiung 2020a). A layer of clay was found at 6.5 m to 8.0 m below ground level, and thicker cohesive materials were found below 18 m of ground depth; these features may explain the value of this ratio. However, such large- scale cofferdam excavation is the only case that could be selected in the city centre of Kaohsiung. The excavation is located at the junction of two main roads, and the displacements are comparatively small. The reliability of the measured surface settlement data is an important consideration due to the magnitude of displacement and the measurement error caused by heavy traffic on the road, and other similar cases in similar ground shall be examined in the future on to confirm the statements made above.

Furthermore, an unexpected additional drawdown of the ground water pore pressure is recognized as a high-level risk, because this might lead to an imbalance of the pressure between the inside and the outside of the excavation zone, causing an excessive settlement of the adjacent ground and structures outside the excavation. Thus, to ensure that there is no unexpected pore pressure change during the excavation, a series of pumping tests were conducted. Figure 8(a) illustrates the locations of the pumping and observation wells for one pumping test performed before the start of the excavation. Figure 8(b) reveals stable water levels in three observational wells (Ows) within the excavation zone, and limited changes occurred in those Ows. Because the locations of these 3 Ows were at certain distances from the pumping well and it was only a single well pumping test, there were very few impacts on the adjacent ground, although the 3 Ows were within the excavation zone.

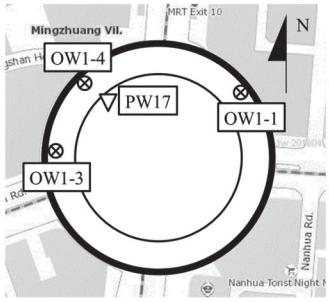

Type	Legend	Name	Depth (m)
Observation wells inside the excavation	⊗	OW1-1	30
		OW1-3	30
		OW1-4	30
Pumping well	▽	PW17	30

(a) Locations and depths of pumping wells, observation wells, and electrical piezometers on site

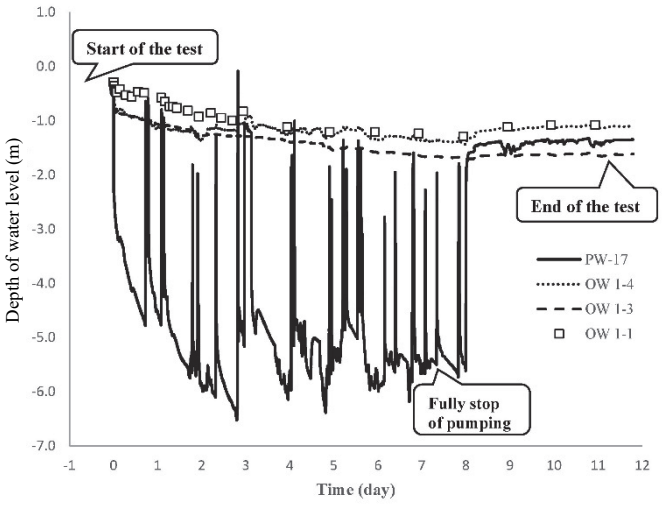

(b) Record of pumping test

Fig. 8 Details of pumping test before start of the excavation

4. NUMERICAL SIMULATION

First, a numerical simulation was performed using the FEM software SEEP/W to simulate the maximum drawdown caused by the pumping of a single well. Table 2 shows the input parameters used for the analyses and 2-dimensional symmetric analyses were undertaken. The horizontal boundaries at the far end from the excavation and the bottom of the model are set to allow ground water to continue to flow into the model but not at the centre of the excavation. The vertical boundary is set at 70 m below surface level associated with available site investigation information. Three thick layers of silty sand with several thin layers of clay are present in the model. The location of pumping well is assumed at the centre of the excavation. Figure 9(a) shows that the observed and simulated results are similar, which could provide a very good reference for determining the pumping details during the main excavation process and also confirms that the permeability of sand shall be in the range of 3 to 4.5×10^{-6} cm/sec. Figure 9(b) shows the piezometric levels both inside and outside the excavation; the piezometric level inside the excavation continued to drop gradually during the excavation, but the changes in the piezometric levels outside the excavation zone became insignificant during the same period. The diaphragm wall outside the pit and the thick, impermeable clay layer at the depth of the wall toe prevented impacts on the ground water pore pressure outside the excavation zone, although pumping was still ongoing inside the area of excavation.

Second, 2-dimensional analyses were undertaken to evaluate the lateral wall deformations induced by the excavation, and the FEM software PLAXIS was adopted. An axis-symmetric simulation was conducted after the excavation, and the model used is presented in Fig. 10. The study aims to validate soil parameters for 2 different soil constitutive models used for excavations in Kaohsiung, except the examination of induced lateral wall displacement. The two models used here are the linear elastic-perfect plastic Mohr-Coulomb (MC) model and a model that includes additional characteristics of unloaded-reloaded behaviours of soils named "Hardening Soil (HS)". Referring to Hsiung *et al*. (2016), the soil parameters for the MC model are presented in Table 3.

For the HS model, additional parameters including E_{50}^{ref}, E_{oed}^{ref} and E_{ur}^{ref} are needed, and these parameters are interpreted from the effective lateral earth pressure and E_{50}, E_{oed} and E_{ur}, respectively. The definition of E_{50}^{ref}, E_{oed}^{ref} and E_{ur}^{ref} is "Reference secant stiffness from drained triaxial test", "Reference tangent stiffness for oedometer primary loading" and "Reference unloading/reloading stiffness", respectively. Details of E_{50}, E_{oed} and E_{ur} have been explained by Plaxis (2016). In a study of tunnelling in similar ground, Hsiung (2020b) suggested that

$$E = 1.5\ E_{50} \quad (1)$$

$$E_{50} = E_{oed} \quad (2)$$

$$E_{ur} = 3E_{50} \quad (3)$$

where E is the initial elastic modulus of soil (Hsiung *et al*. 2016).

Table 2 Inputs of flow quantity prediction using SEEP/W

Number of layer	Soil type	Depth (m)	Permeability (cm/sec)
1	Silty sand	0.0 ~ 6.5	4.50×10^{-3}
2	Low plasticity clay	6.5 ~ 8.0	3.00×10^{-6}
3	Silty sand	8.0 ~ 18.0	4.50×10^{-3}
4	Low plasticity clay/silt with silty sand	18.0 ~ 27.5	1.75×10^{-4}
5	Low plasticity clay/silt with silty sand	27.5 ~ 37.0	1.75×10^{-4}
6	Low plasticity clay/silt with silty sand	37.0 ~ 46.5	1.75×10^{-4}
7	Silty sand	46.5 ~ 58.5	1.50×10^{-3}
8	Low plasticity clay	58.5 ~ 70.0	3.00×10^{-6}

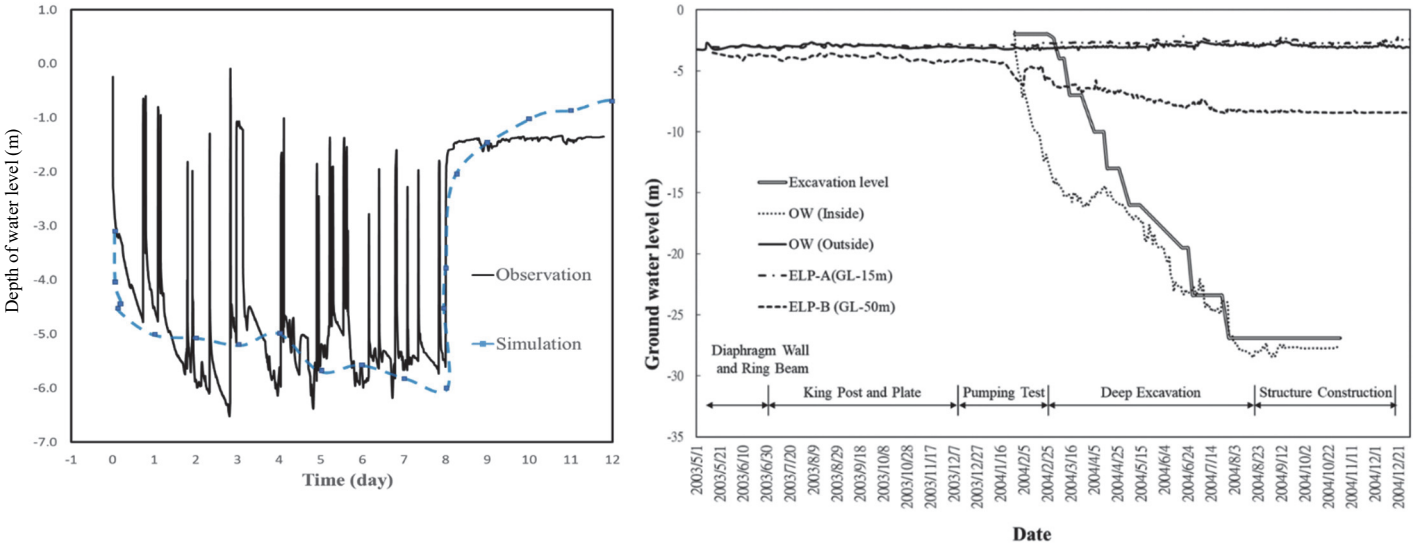

(a) A comparison between the simulation and observation of change of water level of pumping test

(b) Change of water levels inside and outside the excavation during the excavation

Fig. 9 Details of pumping test from simulation and observation and also change of water levels inside and outside the excavation from observations

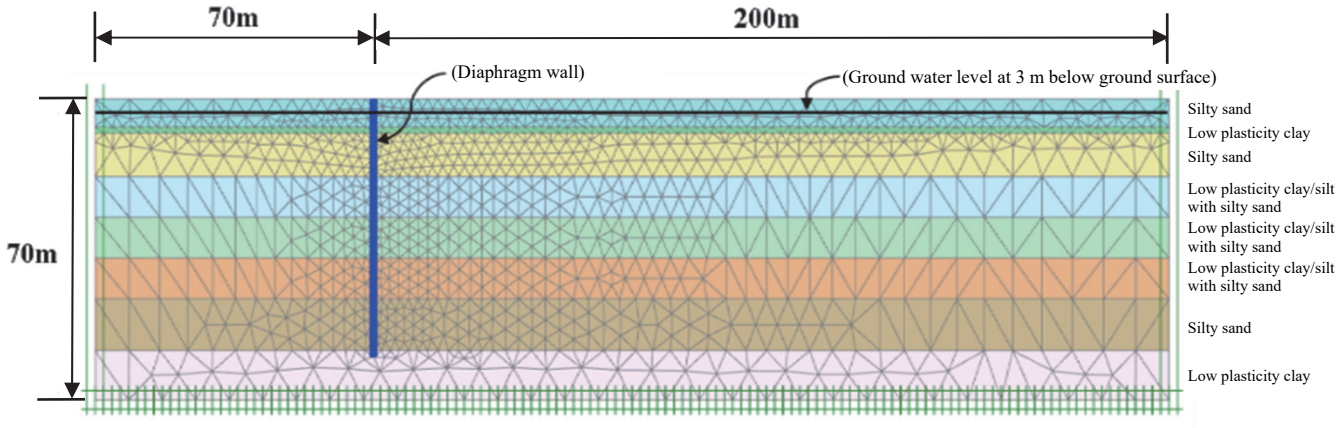

Fig. 10 Numerical model used for simulation of cofferdam excavation

Table 3 Key soil parameters used for simulation using MC model only

(a) Sand

Number of layer	Soil type	Depth (m)	γ_t (kN/m^3)	c' (kPa)	ϕ' (°)	E' (kPa)*
1	Silty sand	0.0 ~ 6.5	19.0	0.2	32	8,500
3	Silty sand	8.0 ~ 18.0	18.8	0.2	32	14,000
7	Silty sand	46.5 ~ 58.5	19.5	0.2	36	28,000

* The Poisson's ratio is assumed to be 0.3.

(b) Silt and clay

Number of layer	Soil type	Depth (m)	γ_t (kN/m^3)	Undrained shear strength, s_u (kPa)	E' (kPa)*
2	Low plasticity clay	6.5 ~ 8.0	19.0	51	9,180
4	Low plasticity Clay/Silt with silty sand	18.0 ~ 27.5	18.8	89	16,094
5	Low plasticity Clay/Silt with silty sand	27.5 ~ 37.0	19.5	118	21,287
6	Low plasticity Clay/Silt with silty sand	37.0 ~ 46.5	19.5	147	26,481
8	Low plasticity clay	58.5 ~ 70.0	22.0	254	44,027

* The Poisson's ratio is assumed to be 0.35 and "Undrained B" analyses are selected.

Table 4 presents the soil parameters used for the HS model in the analyses, but the constitutive model is adopted for sand only due to the limitations of the availability of soil parameters. For cohesive soils such as silt and clay, the MC model is still applied. Table 5 shows the structural parameters, which were used for both the MC and HS models. It is also aware of the analysis using MC model for both sand and clay is undertaken too for a comparison purpose.

The results from both the observations and simulations of lateral wall movements are compared at various stages in Fig. 11 with reliable field data from an inclinometer (SID02). With the exception of the 1st stage of excavation (excavation to 4 m below ground level), the maximum wall displacement was very similar, but in general, the wall displacement beneath the excavation level was significantly over-estimated regardless of the constitutive model used. It is likely that the small strain behaviour of the soil could not be considered in the constitutive model used, which led to an over-estimation of the wall displacement caused by the excavation. Moreover, very thick cohesive soil was observed on the site, and thus the soil behaviours are fully governed by the MC model. Consequently, the results of the simulations are nearly identical for the MC and HS models. As the use of constitute model with small-strain characteristic could perform better for the prediction of wall displacement beneath excavation level (Orazalin *et al*, 2015 and Nikolinakou *et al,* 2011), it is thus recommended that a more advanced model considering small-strain soil behaviour be selected

Table 4 Key soil parameters used for simulation using MC and HS models

(a) Sand (HS model)

Number of layer	Soil type	Depth (m)	γ_t (kN/m^3)	c' (kPa)	ϕ' (°)	E_{50} (kPa)*
1	Silty sand	0.0 ~ 6.5	19.0	0.2	32	5667
3	Silty sand	8.0 ~ 18.0	18.8	0.2	32	9333
7	Silty sand	46.5 ~ 58.5	19.5	0.2	36	18667

* The Poisson's ratio is assumed to be 0.3.

(b) Silt and clay (MC model)

Number of layer	Soil type	Depth (m)	γ_t (kN/m^3)	Undrained shear strength s_u (kPa)	E' (kPa)*
2	Low plasticity clay	6.5 ~ 8.0	19.0	51	9180
4	Low plasticity silt/clay with silty sand	18.0 ~ 27.5	18.8	89	16094
5	Low plasticity silt/clay with silty sand	27.5 ~ 37.0	19.5	118	21287
6	Low plasticity silt/clay with silty sand	37.0 ~ 46.5	19.5	147	26481
8	Low plasticity clay	58.5 ~ 70.0	22.0	254	44027

* The Poisson's ratio is assumed to be 0.35 and "Undrained B" analyses are selected.

Table 5 Structural parameters of the wall used for analyses

Wall thickness (m)	w (kN/m^3)$^+$	EI^* (10^4 kN/m)	EA^* (10^4 kN/m)	Poisson's ratio, μ
1.8	5.5	1055.72	3910.06	0.15

$^+$ "w" means the buoyancy unit weight of the diaphragm wall.

* "E" means elastic modulus of the diaphragm wall and it is assumed to be 2712.3×10^4 kPa; "I" is the moment of inertia of the wall and "A" is the area of cross section of the wall in unit length.

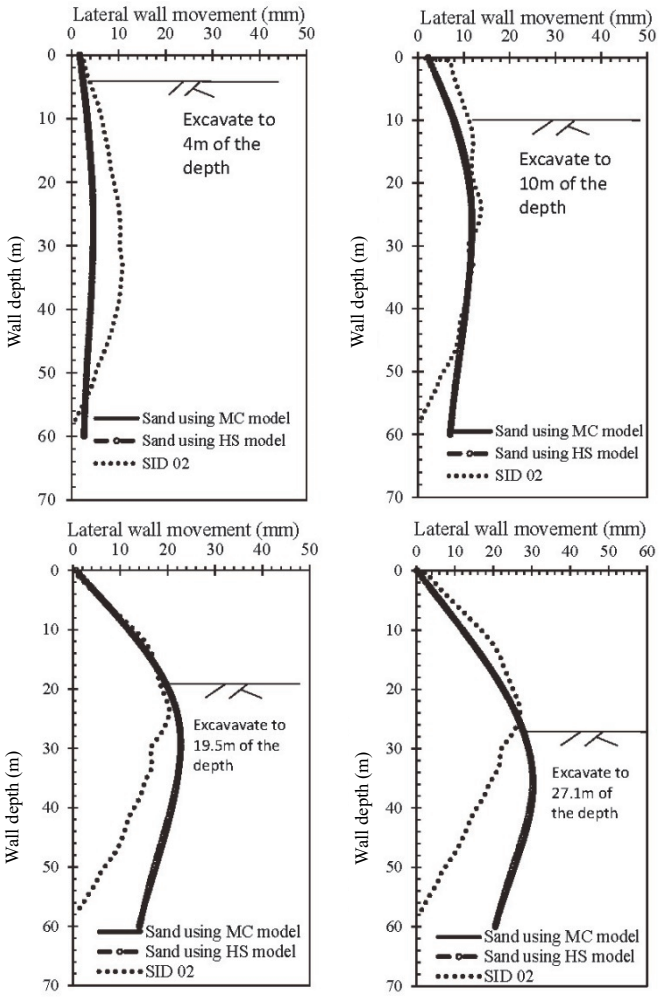

Fig. 11 A comparison of results from observations and simulations in the aspect of lateral wall displacement for at various stages of the excavation of O5/R10

for subsequent simulations to predict excavation-induced displacements more precisely.

Similarly, the surface settlement measured from two comparatively reliable monitoring sections at 2 different excavation stages are compared with the results from the numerical analyses in Fig. 12. The measurements differ significantly from the results of the numerical analyses, regardless of whether the MC or HS model was used, although the prediction using the HS model seems to be slightly better. Hsiung and Dao (2015) indicated that the excavation-induced surface settlement cannot be predicted well when the MC model is adopted. Based on the FEM simulation, it indicates that still up to 4 mm of surface settlement found at approximately 3 times of the maximum excavation depth (around 90 m from the excavation) and 2 mm of surface settlement found at 4 times of the excavation depth (around 120 m from the excavation) at final excavation stage so the influence zone of the excavation is around 3 to 4 times of the excavation depth but as presented in Fig. 12, it is likely that limited impacts from induced surface settlement is seen on the ground around 2 times than the maximum excavation depth. As discussed previously in this study, the simulated behaviours are mainly dominated by the MC model, and thus the conclusions from the comparison are consistent with those of Hsiung and Dao (2015). Again, it is recommended that a more complicated model

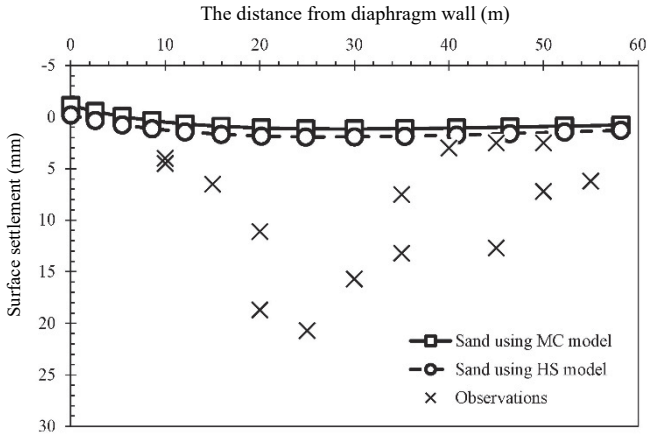

(a) At 1st excavation stage (observed data from SSI-NW1 and SSI-NW2)

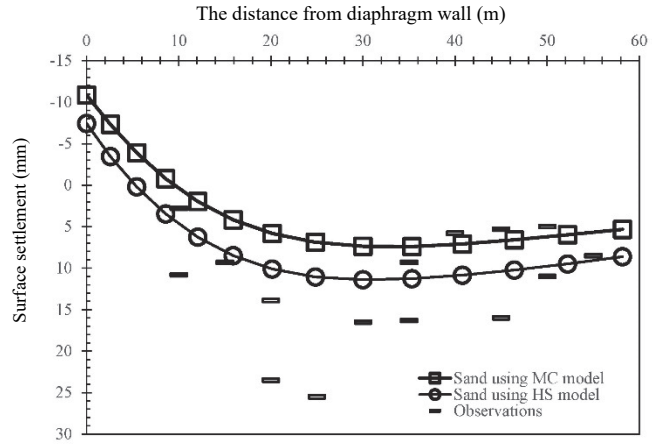

(b) At final excavation stage (observed data from SSI-NW1 and SSI-NW2)

Fig. 12 A comparison of results from observations and simulations in the aspect of surface settlement of O5/R10

with consideration of the small-strain behaviour of soil be applied to obtain a better prediction of surface settlement. This conclusion is also in line with the conclusions of Hsiung and Dao (2015). However, as surface settlements are measured from the surface on the main road, as indicated by Hsiung (2020a), additional factors, such as reliability of instrument installation and survey and also impact from traffic from main road may also affect the measured data which have to be considered.

5. CONCLUSIONS

The completion of phase 1 of the KMRTS provides a better view of the design and construction of large-scale underground structures in highly permeable ground with a high ground water level, which represent conditions that are rarely seen around the world. Thus, the following conclusions were drawn from this study.

1. Studies of excavations in loose to medium dense sands with high ground water levels are relatively rare. In this study, a strut-free cofferdam excavation in this type of ground that was 140 m in diameter and 27 m in depth was selected as the research background. The pit was fully retained by a 1.8-m-thick, 60-m-deep diaphragm wall, and the cofferdam excavation was circular in shape, in contrast to the commonly constructed rectangular shape. To fulfil the requirements for the shape of the excavation, a trench-cutter (EXM) machine was chosen to build the diaphragm wall instead of the hydraulic-grab machine more popularly used in Taiwan.
2. Details of the design and risk analyses of said cofferdam excavation are briefly described, and the key risks of this excavation include (1) an unexpected eccentric load on the retaining wall from the soils; (2) defects or long delays in retaining wall construction; (3) additional drawdown of the ground water level outside of the excavation zone; (4) launching of the tunnel boring (shield) machine; and (5) excessive water ingress from leakage of the wall or unexpected large displacements of the wall.
3. Construction activity was either excluded or severely limited outside the cofferdam to maintain the hoop effect during the excavation. The excavation presented in this paper included lateral wall displacement, surface settlement and changes in pore pressure inside and outside the excavation.
4. Up to 30 mm of the maximum lateral movement occurred at the end of the excavation, and the ratio of the maximum wall displacement to the excavation depth was only 0.11%. The displacement was comparatively small, and it is anticipated that this small ratio is due to the arching effect from cofferdam excavation, the thicker and stiffer wall, and the longer embedded depth.
5. Observations of surface settlement induced by the excavation revealed that the displacements and, for similar reasons, lateral wall displacements were smaller than expected. Ground water levels remained stable during most of the construction period. As the diaphragm walls were embedded deeply into impermeable soils, the cut-off of inflow of ground water during excavation is the reason for the small magnitude of these displacements.
6. Numerical analyses of simulations of both pumping and ground displacements of the cofferdam excavation were performed, which validated that the permeability of sand is in the range of 3 to 4.5 $\times$ 10^{-6} cm/sec. The simulations of ground displacements could predict the maximum wall displacements successfully when the two constitutive models selected in this study were used, except in the 1st excavation stage. However, in general, the wall displacement beneath the excavation level was significantly overestimated, regardless of whether the MC or HS model was used. Furthermore, comparatively worse predictions of surface settlement troughs were obtained, although the prediction using the HS model generated slightly better results. As comparatively thicker cohesive soils were observed onsite and only the MC model was selected for the simulation of cohesive soils due to the absence of soil parameters, it is likely that the overall soil behaviours are dominated by the MC model in this study. An advanced constitutive model with consideration of the small-strain behaviour of soils is recommended to improve the prediction of ground displacements during excavation but influence on measured surface settlement from additional factors, such as the reliability of instrument installation and traffic from main road have to be considered.

ACKNOWLEDGEMENTS

The authors would like to thank to Ms. Maggie Kao, Mr. Jeff Tsai and Mr. Cheng-Lun Tsai, students of National Kaohsiung

University of Science and Technology for their efforts for preparing necessary tables and figures used in this paper.

FUNDING

The authors received no funding for this work.

DATA AVAILABILITY

The data used in this study are not publicity available. They are used in this study under permission from Kaohsiung Mass Rapid Transit Engineering Bureau.

CONFLICT OF INTEREST STATEMENT

The authors declare that there is no conflict of interest.

REFERENCES

Clayton, C.R.I. (2001). *Managing Geotechnical Risk: Improving Productivity in UK Building and Construction*, Thomas Telford, London, UK.

Clough, G.W. and O'Rourke, T.D. (2003). "Construction-induced movement of in situ walls. Design and performance of earth retaining structures." *ASCE Special Publication*, **25**, 439-470.

Hsiung, B.C.B. (2020a). "Observations of the ground and structural behaviours induced by a deep excavation in loose sands." *Acta Geotechnica*, **15**(6), 1577-1593. https://doi.org/10.1007/s11440-019-00864-0

Hsiung, B.C.B. (2020b). "Numerical investigation of the three- dimensional performances of a shield-machine-bored tunnel in loose sands," *Soil Mechanics and Foundation Engineering*, February issue, published by Springer, **56**, 427-435. https://doi.org/10.1007/s11204-020-09626-7

Hsiung, B.C.B. and Dao, S.D. (2015). "Prediction of ground surface settlements caused by deep excavations in sands." *Geotechnical Engineering*, **46**(3), 111-118.

Hsiung, B.C.B., Yang, K.H., Wahyuning, A., and Hung, C. (2016). "Three-dimensional effects of a deep excavation on wall deflections in loose to medium dense sands." *Computers and Geotechnics*, **80**, 138-151. https://doi.org/10.1016/j.compgeo.2016.07.001

Nikolinakou, M.A., Whittle, A.J., Savidis, S., and Schran, U. (2011). "Prediction and interpretation of the performance of a deep excavation in Berlin sand." *Journal of Geotechnical and Geoenvirnmental Engineering,* ASCE, **137**(11), 1047-1061. http://doi.org/10.1061/(ASCE)GT.1943-5606.0000510

Orazalin, Z.Y., Whittle, A.W., and Olsen, M.B. (2015). "Three-dimensional analtses of excavation support system for the State Centre basement on the MIT campus." *Journal of Geotechnical and Geoenvirnmental Engineering*, ASCE, **141**(7), 0501500. https://doi.org/10.1061/(ASCE)GT.1943-5606.0001326

Ou, C.Y., Hsieh, P.G., and Chiou, D.C. (1993). "Characteristics of ground surface settlement during excavation." *Canadian Geotechnical Journal*, **30**(5), 758-767. https://doi.org/10.1139/t93-068

PLAXIS. (2016). *Reference Manual*, Amsterdam, The Netherlands: Plaxis BV

Puller, M. (2003). *Deep Excavations: A Practical Manual*, Thomas Telford, London, UK.

Skempton, A.W. (1986). "Standard penetration test procedures and the effects in sands of overburden pressure, relative density, particle size, ageing and overconsolidation." *Géotechnique*, **36**(3), 425-447. https://doi.org/10.1680/geot.1986.36.3.425

Yao, R.C. (2005). *Engineering Performance of Deep Excavation in Kaohsiung – Using Case Histories of O6, O7 and O8 Station in Kaohsiung Metro,* M.Sc. Thesis, National Kaohsiung University of Applied Sciences, Taiwan (in Chinese).